Environmental and Ecological Statistics **11,** 257–281, 2004

Spatial analysis of semi-arid patchy vegetation by the cumulative distribution of patch boundary spacings and transition probabilities

R. WEBSTER[1] and F.T. MAESTRE[2]*

[1]*Rothamsted Research, Harpenden, Hertfordshire AL5 2JQ, UK*
E-mail: richard.webster@bbsrc.ac.uk
[2]*Departamento de Ecología, Universidad de Alicante, Apartado de correos 99, 03080 Alicante, Spain*

Received December 2001; Revised November 2003

The vegetative cover in semi-arid lands typically occurs as patches of individual species more or less separated from one another by bare ground. We have adapted two methods to quantify the spatial pattern of such cover from measurements across patches on transects.

Transects were laid in several directions across digital maps of the land surface or across the land itself, and the distances between successive patch boundaries were measured. The distances were ranked in order, and their cumulative distributions were computed and modeled with gamma functions. The parameters of the model provided estimates of the mean distance across patches. The means for different directions were further tested for anisotropy. Transitions between classes on the transects estimate the probabilities with which the different species occur next to others (and to bare ground) and so describe the arrangement of the patches occupied by the different species.

The methods were tested with data from mosaic patterns at three semi-arid sites dominated by the tussock grass *Stipa tenacissima*. The differences in the estimated mean boundary spacings from site to site accorded with prior qualitative assessment, as did the estimated anisotropy. The transition matrices and the estimated proportions of cover showed the dominance of the bare soil with which all the individual species are intimately associated. The transitions also suggest the presence of both positive and negative relations among the main species. Those between *Stipa tenacissima* and *Brachypodium retusum* seem to be facilitative, as do those between this grass and the shrub *Anthyllis cytisoides*. In contrast, *Globularia alypum* seems to inhibit the other species.

We also estimated transition probabilities geostatistically by summing the indicator variograms of the individual species. Standard variogram models were then fitted to describe the ordered series of values, and these again produced results that accorded with visual impressions.

Keywords: gamma function, geostatistics, spatial pattern, maps, mosaic vegetation, *Stipa tenacissima*, semi-arid

*Present address: Department of Biology, Duke University, Box 90340, Durham, North Carolina 27708-0340, USA. E-mail: maestre@duke.edu.

1352-8505 © 2004 Kluwer Academic Publishers

1. Introduction

The vegetation of semi-arid lands typically occurs as patches of individual species more or less separated from one another by bare ground. In this arrangement the plants can survive on scarce rainfall by restricting transpiration on a fairly small proportion of a catchment while exploiting all the water beneath the soil and by intercepting runoff from the bare ground between them. The notion has led HilleRisLambers *et al*. (2001), for example, to model the genesis of patchy patterns by their interaction with soil water and its dynamics.

Before one can explain and model the behavior of the vegetative cover one needs a description of that cover. The proportion of the ground covered is an obvious attribute of it, but so are the sizes of patches, the interactions between species, and any orientation of the pattern. These attributes have important roles in the dynamics of semi-arid ecosystems (Aguiar and Sala, 1999).

Describing the spatial distributions of vegetation quantitatively has a long history. It has included the analysis of point patterns of individual plants (Diggle, 1983; Dale, 1999), variance : mean ratios at different resolutions determined from quadrats of varying size (Greig-Smith, 1983), quadrat variance methods (Pielou, 1977; Dale and Blundon, 1990), spectral analysis (Platt and Denman, 1975), and more recently wavelets (Bradshaw and Spies, 1992), each having merit in appropriate circumstances. Most of these methods are designed to analyze spatially located points or data collected from line intercept sampling or grids of contiguous quadrats, and their application to describe the spatial pattern of semi-arid patchy vegetation is not always possible. The use of point pattern methods is not suitable for studying communities in which individuals are not easily distinguished (Diggle, 1983; Dale, 1999), such as two-phase mosaics of vegetation in semi-arid regions. Quadrat variance methods require a lot of work to collect the data in two dimensions, and it is difficult to detect anisotropy by them (Dale, 1999). Two-dimensional spectral analysis can satisfactorily detect fairly regular patterns and estimate their periods and anisotropy (Ford and Renshaw, 1984), but, as Dale (1999) points out, one must treat the observed patterns as outcomes of processes that are stationary throughout the region sampled.

The nature of the task that confronts us, that of reducing the complex pattern of patchy vegetation of multiple species communities to appropriate summary statistics and descriptive visualizations without loosing too much information, is best explained with reference to Figs 1 and 2. In Fig. 1 are two photographs of such cover, the second of which when viewed from above can be mapped as in Fig. 2. This map shows to scale the individual patches, with each species designated by its own unique ornament, amidst bare soil. The patches are seen to be bounded, and of varying size. Some are completely surrounded by bare soil, some touch other patches of different species, and some appear to be preferentially oriented along the contour. A technique that seems to us well suited for the spatial analysis of this kind of vegetation is one devised originally by Burgess and Webster (1984) for analyzing patterns of soil, which also occur in patches of different types. It was pursued successfully by Müller and Böttcher (1987), also for describing soil patterns. The method can be used directly in the field, with aerial photographs, conventional maps and digital maps at various scales. It involves placing transects across a region or a detailed map of it, recording where the transects cut the boundaries of the patches and the species composing the patches, and then analyzing the results.

The particular community that interests us is the tussock-grass steppe dominated by

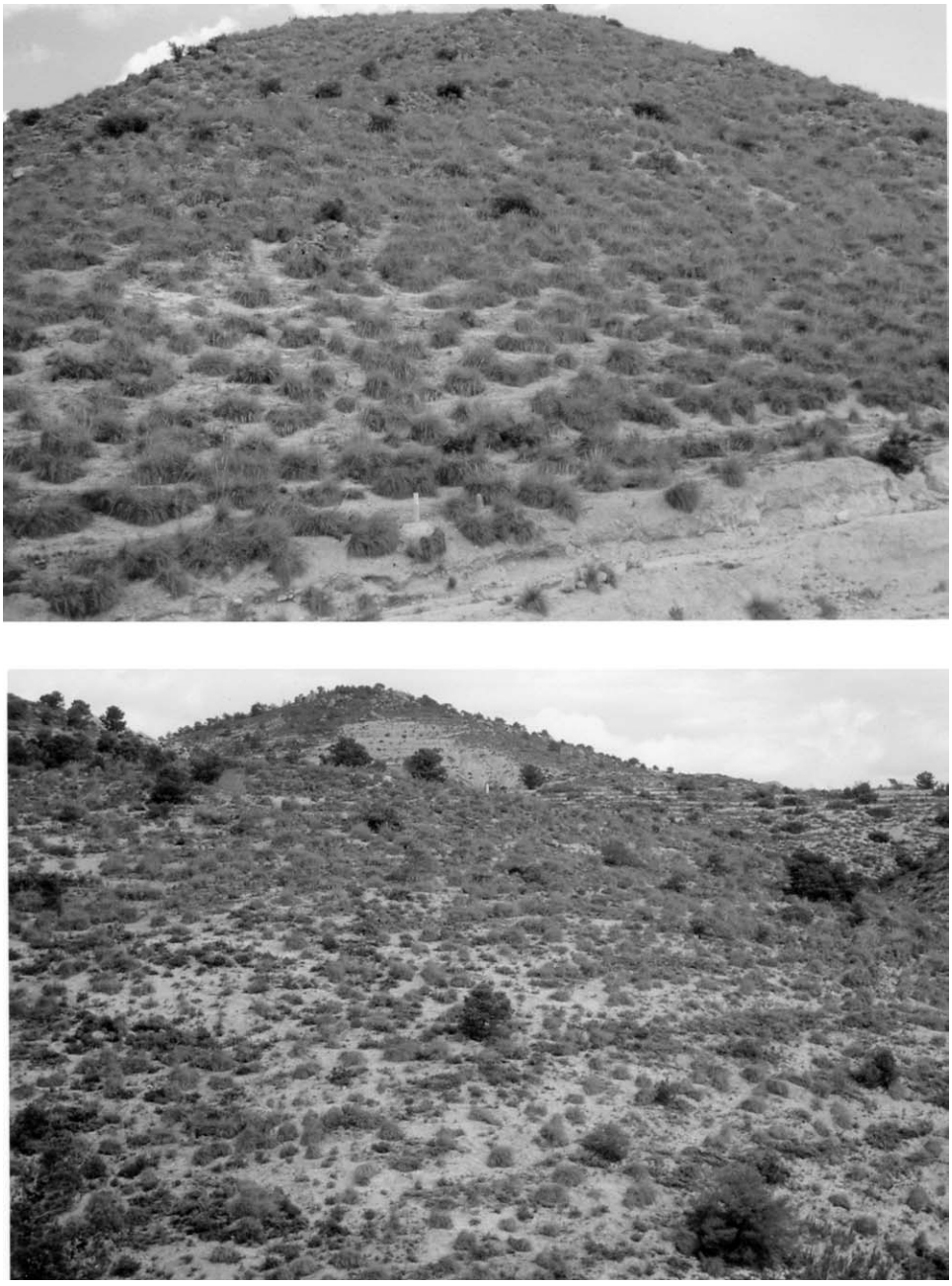

Figure 1. Photographs of the *Stipa tenacissima* tussock steppe at Marquesa (upper photograph) and Aguas (lower photograph).

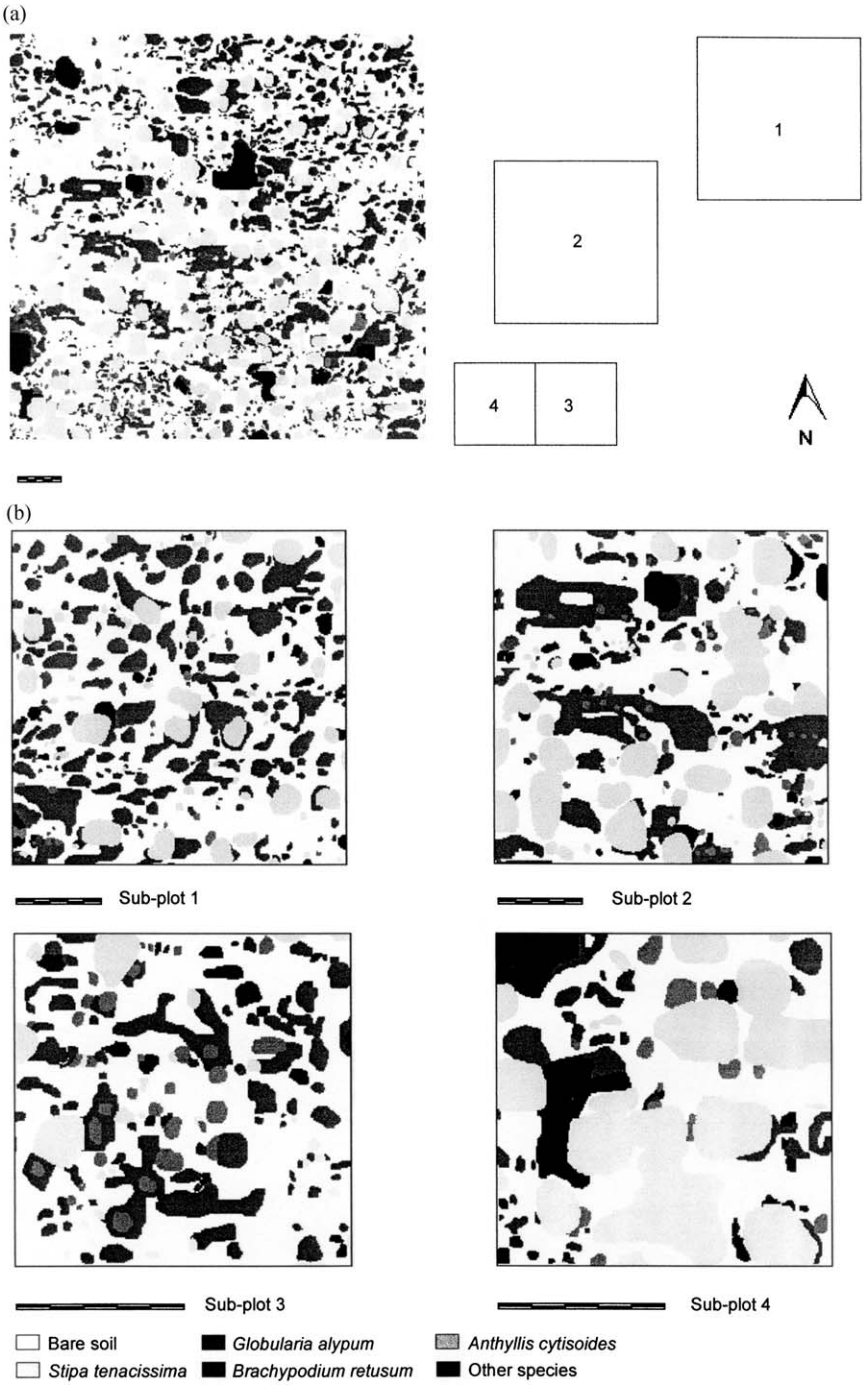

Figure 2. (a) Map of the whole plot at Aguas (on the left) with the patches of the principal species distinguished and the four sub-plots demarcated (on the right). (b) Maps of the four sup-plots. Scale bar represents 5 m in all cases.

esparto or alpha grass (*Stipa tenacissima* L.). It is widespread in the semi-arid parts of the Mediterranean Basin where it covers some 4000 km^2 in Southern Europe (Ministerio de Medio Ambiente, 1999), and more than 60 000 km^2 in North Africa (Le Houérou, 1986). The characteristics and distribution of the vegetated patches in this community affect the interception of rain and control the flow of runoff and sediment (Puidefábrigas and Sánchez, 1996; Cammeraat and Imeson, 1999), which in turn are essential for maintaining the vegetation (Aguiar and Sala, 1999).

We have explored the application of the method of Burgess and Webster (1984) to characterize statistically the spatial patterns of *S. tenacissima* steppes and to analyze the interspecific relations among vegetated patches. We tested it using data obtained from digital maps and direct field mapping in three small regions of the steppe in south-east Spain. We report the results and discuss their possible implications for ecosystem dynamics. As far we know, the technique has not been applied to vegetation, and we explore its value here.

2. Study area and sampling

We explain the method in relation to a particular case study, and so we describe the sites and their vegetation first.

2.1 *The sites*

We chose three sites on which to study the pattern of the vegetation, all in the province of Alicante, in south-east Spain. They are ''Aguas'' (38°31′N, 0°21′W, 461 m above sea level), ''Marquesa'' (38°27′N, 0°24′W, 170 m above sea level), and ''Hotel'' (38°29′N, 0°23′W, 290 m above sea level). The climate there is semi-arid, with a mean annual rainfall less than 350 mm, hot dry summers, and mean annual temperatures of 16–18°C (Pérez Cueva, 1994). All three sites are on moderate slopes (12° at Aguas, 23° at Marquesa, and 17° at Hotel), and all face south. The soil is stony and calcareous, and at the Hotel site there are numerous strips of rock outcropping approximately from north-west to south-east.

The vegetation is an open steppe of the *Lapiedro martinezii–Stipa tenacissimae* community and occurs as distinct patches (Fig. 1). Those of the alpha grass, *S. tenacissima* L. and the herb *Brachypodium retusum* (Pers.) P. Beauv. dominate; less frequent are the shrubs *Globularia alypum* L., *Anthyllis cytisoides* L., *Ephedra fragilis* Desf., and *Rhamnus lycioides* L. These, and the few individuals of other species, cover about 45% of the ground. The remainder of the ground is bare soil. The whole makes a mosaic. Fig. 2a, a map of the Aguas site, is one example.

2.2 *Sampling and measurement*

At Aguas we took a 0.25-ha (50 m × 50 m) square and divided it into 2500 1 m × 1 m quadrats. All the perennial vegetation was accurately mapped in each quadrat in the spring of 1999. The maps of the individual quadrats thus drawn were scanned electronically and

assembled into a single map of the square with Photoshop 5.0 (Adobe Systems Inc., San José, CA, USA) to give Fig. 2a. At the Marquesa and Hotel sites we recorded the vegetation directly in the field on 0.0625-ha (25 m × 25 m) squares in the autumn of 2000.

One immediately evident feature of Fig. 2a is that some portions of the site are dominated by small patches, whereas in others the patches are large on average. We want our method to distinguish these. In like manner, we want the method to distinguish the sites at Marquesa and Hotel on the general coarseness of the patterns. We also note that some of the patches are distinctly elongated, and if the elongation is in some preferred direction then we should like to have an estimate of that direction and of the degree of elongation. Such anisotropy, if related to the direction of slope, could be another important characteristic of the pattern. As above, parts of the square at Aguas are dominated by large patches, whilst in others the patches are typically smaller. We, therefore, stratified the square into four sub-regions according our perception of the average size of the patches. The positions of the four strata are shown on the right of Fig. 2a, and the patchworks within those strata appear enlarged in Fig. 2b.

Measurements were then made as follows. For the Aguas site we placed sample transects across the map and recorded where the transects cut the boundaries of the patches and the species, or bare ground, composing the patches. We had 20 such transects for the whole plot, each one starting at a random point within the plot. Eight of them were laid out with their directions incremented by 22.5°; the directions of the remaining 12 were chosen randomly. In each of the four sub-plots we had 16 transects, again with random starting points. Of these eight were laid out at regular 22.5° intervals in direction while the other eight were placed in random directions. At the Marquesa and Hotel sites, we laid out the transects (20 at each) directly on the ground and recorded the boundaries in the field. The result was that for each whole plot and for each sub-plot separately at Aguas we had a set of inter-boundary distances on the transects for each species, and for the distances on each individual transect we had the direction also. These constitute our data, which are available from F.T. Maestre on request.

In the event, only four species were sufficiently abundant at Aguas and the Hotel site for us to estimate their contributions to the pattern. They are *S. tenacissima*, *G. alypum*, *B. retusum*, and *A. cytisoides*, which together amount to more than 88% of total plant cover. We grouped all the other species as ‘‘others’’, and the bare soil constituted a sixth class in the mosaic. At Marquesa there were only two common species, namely *S. tenacissima*, and *G. alypum*.

3. Statistical analysis

We observe that the individual tussocks, shrubs and herbs occupy coherent mutually exclusive patches of ground. They may share common boundaries, or they may be surrounded more or less completely by bare soil, which also appears as another group of mutually exclusive patches. The whole makes a mosaic.

Two attributes can be used to describe the pattern. One is some function of the size of the patches, the other is their arrangement relative to one another. We deal with these in order. After that we look at a geostatistical approach to the task and compare the results.

3.1 *Distribution of the distances between successive patch boundaries*

We determined the distribution of the distances between successive patch boundaries within each plot and sub-plot as follows. We ranked the inter-boundary distances from smallest to largest and formed their cumulative distribution. We can plot this distribution against distance, as in each of the graphs in Fig. 3.

In the simplest cases, we might imagine that boundaries occur without regard to one another in a random way. If so then their distribution should be fitted by an exponential function:

$$G(x) = 1 - \exp(-\lambda x), \tag{1}$$

in which x is the separating distance and λ is the intensity of the process. The reciprocal of λ is the mean distance between successive boundaries.

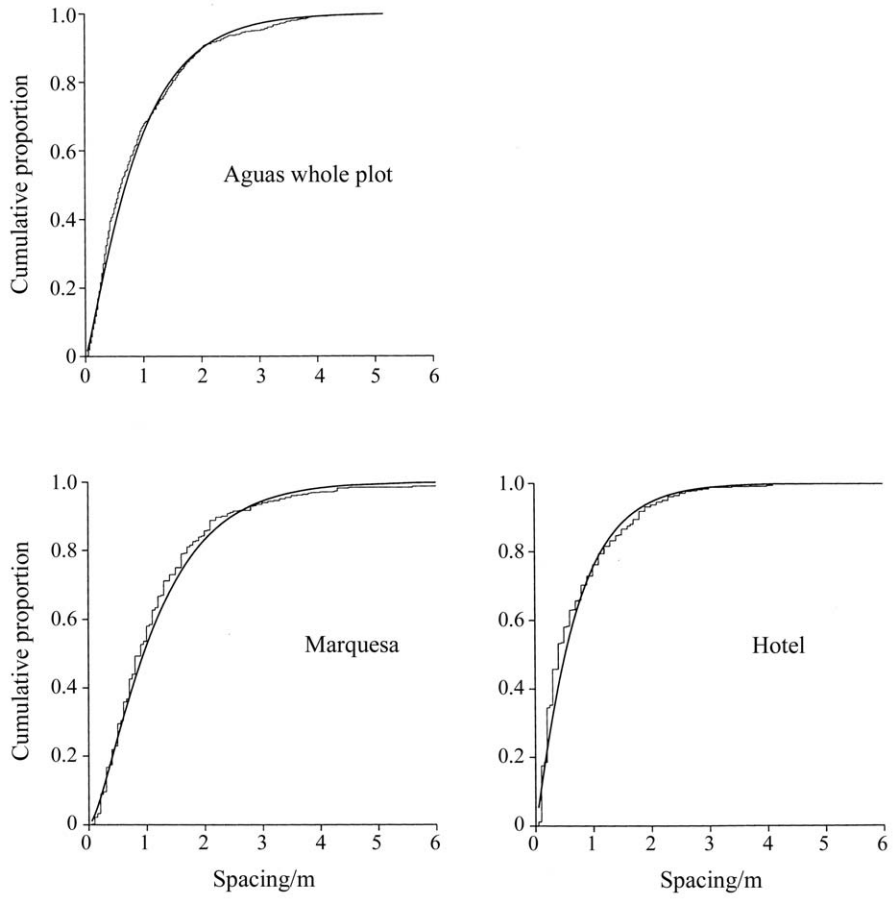

Figure 3. Cumulative distributions of inter-boundary spacings and fitted gamma functions for three main plots.

In practice, we found that on all the plots the small distances are over-represented by this model. Whereas the exponential model has a steadily decreasing first derivative, the observed distributions typically reverse their curvature near the origin, and we have found that the more general gamma distribution fits better and describes the curvature well. The cumulative function is

$$G(x) = \int_0^x \frac{\lambda(\lambda y)^{\alpha-1}}{\Gamma(\alpha)} \exp(-\lambda y)\mathrm{d}y. \tag{2}$$

It has the additional parameter α, for which $\Gamma(\alpha)$ is a constant and from which the distribution gets its name. This quantity is given by

$$\Gamma(\alpha) = \int_0^\infty y^{\alpha-1} \exp(-y)\mathrm{d}y. \tag{3}$$

If $\alpha = 1$ then Equation (2) reduces to Equation (1), and we see that the exponential distribution is a special case of the gamma distribution.

The parameter α describes the shape of the curve, especially near the origin. If $\alpha < 1$ then the function increases more steeply from the origin than does the exponential curve; if on the other hand it is greater than 1 then the curve is sigmoid, and this is what we have found in all the examples we have studied.

3.1.1 Estimating the parameters

The exponential distribution is characterized by the single parameter λ, which we can estimate as the reciprocal of the mean of the distances between successive boundaries, $1/\overline{x}$. Its standard deviation equals the mean. The mean of the gamma distribution is α/λ, and its variance is α/λ^2. So, if $\overline{x}$ and s^2 are, respectively, the mean and variance of the sample then α and λ can be estimated by

$$\widehat{\alpha} = \frac{\overline{x}^2}{s^2}, \tag{4}$$

and

$$\widehat{\lambda} = \frac{\overline{x}}{s^2}. \tag{5}$$

In practice these are poor estimators because they rely on means of very skewed distributions. Maximum likelihood estimates are better, and when based on more than 20 observations they are reliable. This is the method we have used and is described in Burgess and Webster (1984, 1986).

With this procedure, we can estimate the cumulative distribution of the patch boundary spacings for all the classes of the vegetation mosaic. The result is a summary that averages over all classes. We can obtain detail for individual species also by calculating the cumulative distributions for each separately. The result might help us to understand the species' ecological characteristics such as their patterns of growth, their size-class distributions, and age-class distributions. To show what can be done we calculated the cumulative distribution of the patch boundary spacings separately for each of the main species and the bare soil at Aguas.

3.1.2 Anisotropy

As above, patches may be elongated, and if the elongation is in some preferred direction, say ϕ, then the whole pattern can appear anisotropic. We might treat the anisotropy as geometric, such that a simple linear transformation of the geographic space would make the pattern isotropic. If so we have to find the parameters, A, B, and ϕ of an ellipse:

$$\Omega(\theta) = \sqrt{A^2 \cos^2(\theta - \phi) + B^2 \sin^2(\theta - \phi)}, \tag{6}$$

where θ takes values from 0 to 2π, A and B are the long and short diameters, respectively, and ϕ is its orientation, that is, the direction in which A lies. The anisotropy ratio B/A is a measure of the ellipse's eccentricity. Setting the mean first equal to B and then equal A will give the bounds on the model of the distribution function in Equation (2).

3.2 *Transition probabilities*

The second feature of the pattern is the arrangement of the patches occupied by the different species. This arrangement can be described simply by the relative frequencies with which the different kinds of patch occur next to one another on the transects, their transition probabilities. Let us denote the probability that a patch of species j lies next to one of species i as p_{ij}; it is the probability that we shall move from a patch of species i to one of species j on a transect. In general it differs from the probability of moving from a patch of species j to one of species i because the two species do not necessarily share the same neighbors.

We can estimate the transition probabilities from the transects. We simply count the numbers of transitions between class i and class j and divide the result by the total number of transitions involving class i:

$$p_{ij} = \frac{n_{ij}}{\sum_{j=1}^{K} n_{ij}}, \tag{7}$$

where K is the number of different classes or species. The computation is repeated for all K classes, and the results are assembled in a matrix, $\mathbf{P}$, which represents the pattern.

3.3 *A geostatistical approach*

Another approach for quantifying the scale of patchiness lies in combining the transition probabilities with geostatistics and is due largely to Goovaerts (1994) and Goovaerts and Webster (1994). The underlying idea is that the observed pattern is the realization of a random process, $S(\boldsymbol{x})$, with a finite number of states, k, $k = 1, 2, \ldots, K$. In this instance, the K states are the classes of vegetative cover, including bare ground. This spatial process has a transition probability function, defined by

$$\text{Prob}(\boldsymbol{h}) = \text{E}[\text{S}(\boldsymbol{x}) \neq \text{S}(\boldsymbol{x} + \boldsymbol{h})], \tag{8}$$

where $\boldsymbol{x} = \{x_1, x_2\}$ denotes the spatial coordinates of any point and $\boldsymbol{h}$ is the lag, a separating vector in both distance and direction. Thus, Prob($\boldsymbol{h}$) is the probability that the

class of cover at two places a vector $\boldsymbol{h}$ apart are different. The quantity $[S(\boldsymbol{x}) \neq S(\boldsymbol{x}+\boldsymbol{h})]$ defines an indicator, I, taking the value 1 if the states at $\boldsymbol{x}$ and $\boldsymbol{x}+\boldsymbol{h}$ are different and 0 otherwise:

$$I[S(\boldsymbol{x}) \neq S(\boldsymbol{x}+\boldsymbol{h})] = \begin{cases} 1 & \text{if } S(\boldsymbol{x}) \neq S(\boldsymbol{x}+\boldsymbol{h}), \\ 0 & \text{otherwise.} \end{cases} \tag{9}$$

If we have records of the cover at many points, $s(\boldsymbol{x}_l)$, $l = 1, 2, \ldots$, as we have along the transects in our study, then we can estimate Prob($\boldsymbol{h}$) by

$$\widehat{\text{Prob}}(\boldsymbol{h}) = \frac{1}{m(\boldsymbol{h})} \sum_{j=1}^{m(\boldsymbol{h})} i[s(\boldsymbol{x}_j) \neq s(\boldsymbol{x}_j+\boldsymbol{h})], \tag{10}$$

in which the lower case i denotes the indicator of the observations, and $m(\boldsymbol{h})$ is the number of paired comparisons in the summation. In practice this quantity is calculated as the sum of the experimental indicator variograms of the individual cover classes:

$$\widehat{\text{Prob}}(\boldsymbol{h}) = \sum_{k=1}^{K} \widehat{\gamma}_k(\boldsymbol{h}), \tag{11}$$

where

$$\widehat{\gamma}_k(\boldsymbol{h}) = \frac{1}{2m_k(\boldsymbol{h})} \sum_{j=1}^{m_k(\boldsymbol{h})} \{i_k(\boldsymbol{x}_j) - i_k(\boldsymbol{x}_j+\boldsymbol{h})\}^2 \tag{12}$$

is the experimental indicator variogram of the kth class. In this expression, $i_k(\boldsymbol{x}_j)$ is 1 if the cover at $\boldsymbol{x}_j$ is class k and 0 otherwise. The quantity $m_k(\boldsymbol{h})$ is the number of paired comparisons as before.

By varying the lag, $\boldsymbol{h}$, in Equation (10) we obtain an ordered series, like an experimental variogram. Typically the values in the series increase with increasing lag distance, as in Figs 9 and 10 later. This makes sense; we expect that with increasing separation the probability of two points' being in different classes will increase. Also as with a variogram, we can regard the observed series as representing the underlying function in the region and fit a model from one of the legitimate families to it. A probability is necessarily bounded, and so the model we choose will have an effective range beyond which the probability of transition remains sensibly constant. We may interpret this range as the average distance across patches on the transects. The actual models used are described in the next section.

4. Results

4.1 *Aguas whole plot*

Fig. 3 shows the cumulative distribution of the interboundary spacings for the whole of the plot at Aguas, regardless of direction, as the stepped line. The smooth curve is that of the fitted gamma distribution with parameters $\lambda = 1.46$ and $\alpha = 1.35$, giving a mean interboundary spacing of $\bar{x} = 0.924$. The curve is distinctly sigmoid near the origin, a

Table 1. Estimates of the parameters λ (intensity) and α (shape) of the gamma distribution, mean boundary spacing ($\bar{x}$), and the parameters of the ellipses fitted to the anisotropy—maximum and minimum spacings, A and B, the anisotropy ratio (B/A), and the direction of maximum spacing, ϕ, in degrees.

				Anisotropy			
Plot	λ/m^{-1}	α	$\bar{x}/m$	*A/m*	*B/m*	*B/A*	ϕ
Aguas whole plot	1.461	1.350	0.924	0.988	0.887	0.898	156.6
Aguas sub-plots							
1	1.904	1.587	0.833	0.986	0.719	0.729	26.0
2	1.349	1.276	0.946	0.997	0.927	0.930	157.7
3	2.752	1.548	0.563	0.640	0.517	0.808	1.7
4	1.444	1.158	0.803	0.918	0.722	0.786	87.6
Marquesa	1.282	1.533	1.196	1.392	1.165	0.837	171.5
Hotel	1.557	1.113	0.715	0.918	0.640	0.697	123.5

feature resulting from an estimate of α substantially larger than 1 (Table 1). As mentioned above, we analyzed the interboundary spacing for the main species and bare soil separately at Aguas, and Fig. 4 shows the results. There are evidently substantial differences between the species, which are summarized by the fitted parameters listed in Table 2. *Stipa tenacissima* has the largest mean, $\bar{x} = 1.150$, and *A. cytisoides* has the smallest, only 0.344.

By analyzing the transects separately we obtain the 20 curves in Fig. 5a. Evidently the spread is substantial. Some of it we may attribute to sampling fluctuation, and some might represent anisotropy. We have therefore fitted Equation (6) to the means, $\bar{x}$, of the 20 transects using the FITNONLINEAR directive in GenStat (Payne, 2002). The upper graph in Fig. 6 is the result. The maximum and minimum diameters are 0.988 m and 0.887 m, respectively, with an anisotropy ratio of $B/A = 0.898$ and direction of elongation $\phi = 156.5^\circ$ (Table 1). The fit is poor, however, accounting for only about 10% of the variation.

The eccentricity can be translated into the two bold lines in Fig. 5a; these curves are the bounds on the model for which the intensities are 1.40 and 1.53. There is little evidence for anisotropy in Fig. 2 for the whole plot, and we may regard the graph in Fig. 3 and its parameters as a fair summary of the pattern.

Table 2. Estimates of the parameters λ (intensity) and α (shape) of the gamma distribution, and mean boundary spacing ($\bar{x}$) for the four main species, other species, and bare soil at Aguas.

Species	λ/m^{-1}	α	$\bar{x}/m$
S. tenacissima	1.882	1.636	1.150
G. alypum	2.263	4.243	0.533
B. retusum	1.634	2.402	0.680
A. cytisoides	3.384	9.849	0.344
Bare soil	1.235	1.107	1.116
Others	1.560	1.735	0.899

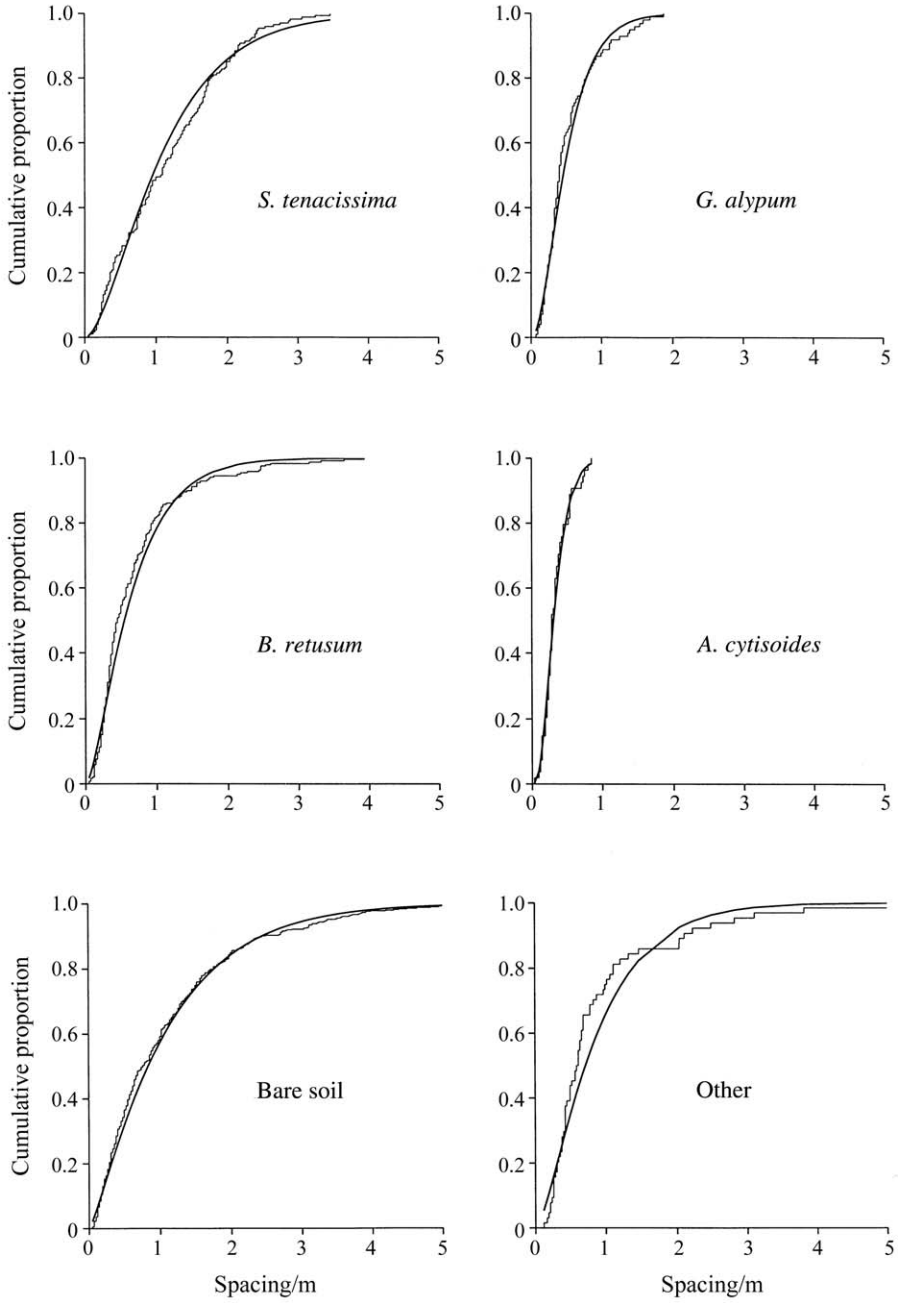

Figure 4. Cumulative distributions of inter-boundary spacings and fitted gamma functions for the four principal species, other species, and bare soil at Aguas.

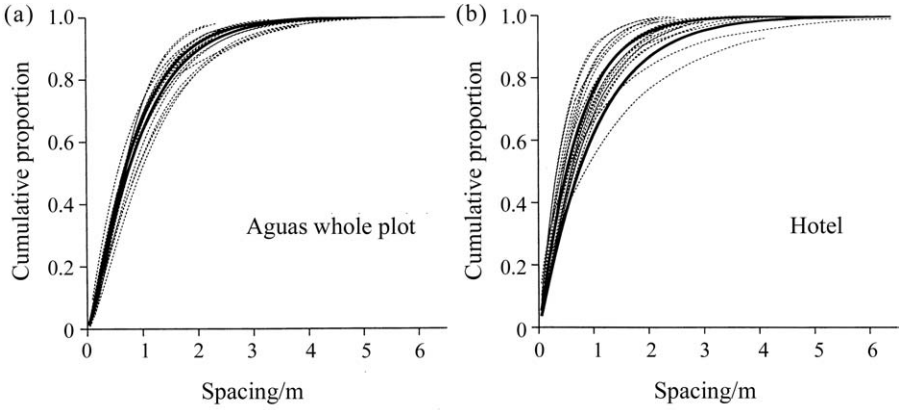

Figure 5. Gamma functions for the 20 separate transects at the Aguas (whole plot) and Hotel plots, with the envelopes of the anisotropy shown by bold lines.

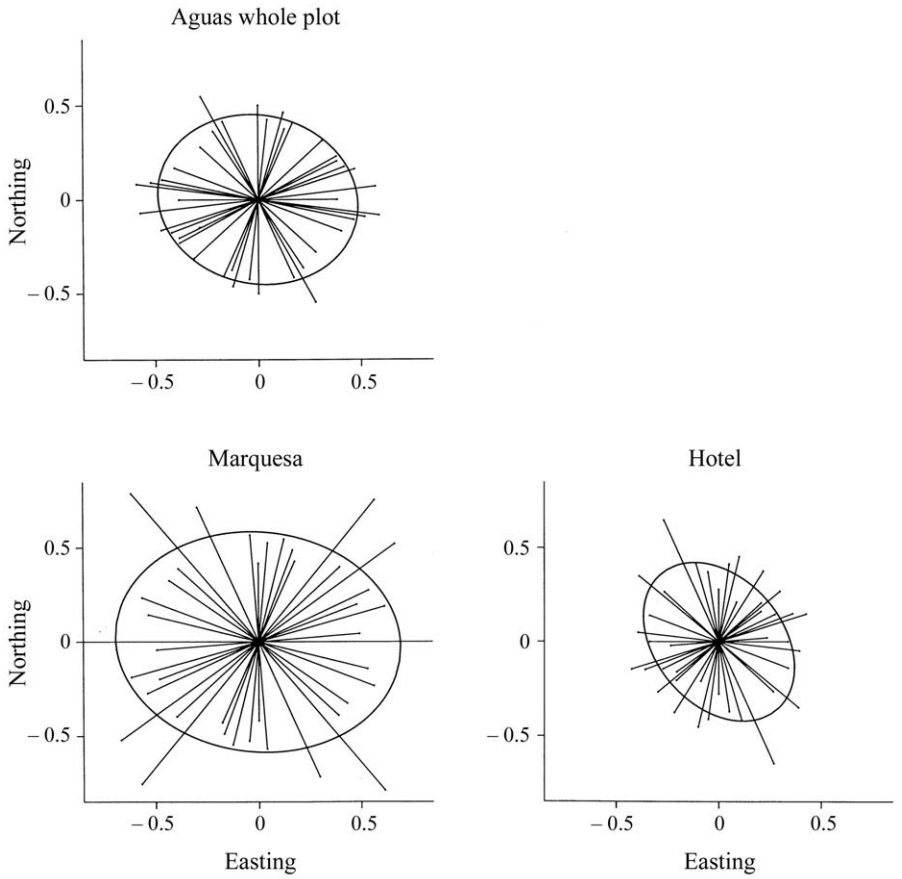

Figure 6. Ellipses fitted to mean spacings of the 20 transects at (a) Aguas, the whole plot, (b) Marquesa, and (c) Hotel.

4.2 *Aguas sub-plots*

Fig. 7 shows the cumulative distributions and fitted curves for the four sub-plots at Aguas. The estimated parameters are listed in Table 1. There are very substantial differences in the means. Sub-plot 2 has the largest mean, $\overline{x} = 0.946$, and sub-plot 3 has the smallest, only 0.563. These accord with what are visibly the coarsest and finest patterns in Fig. 2.

In Fig. 8, we show the mean spacings for the separate directions and the ellipses that we have fitted to them. Again, the small ellipse for sub-plot 3 is a measure of the fine pattern. The apparent anisotropies seem a little surprising. That for sub-plot 1 is believable; many of the patches of *B. retusum* are somewhat elongated in a generally west-to-east direction. The fitted ellipse accounts for 15% of the variance in average spacing, the anisotropy ratio is 0.729, which is substantially different from 1. In sub-plot 2 the patches of *B. retusum* elongated from west to east seem to be matched by ones of *S. tenacissima* elongated from north to south, and the resulting ellipse in Fig. 8 is almost circular. Sub-plot 3 shows some elongation from west to east; the ellipse fitted to sub-plot 4 has its long axis oriented north

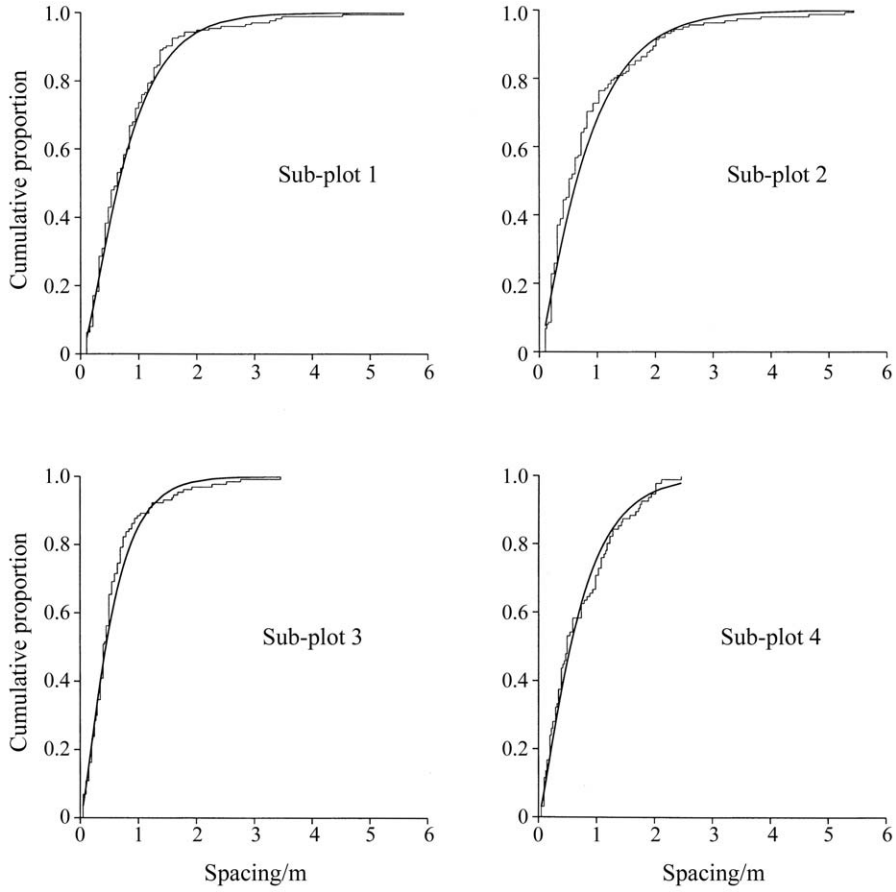

Figure 7. Cumulative distributions of the four sub-plots at Aguas.

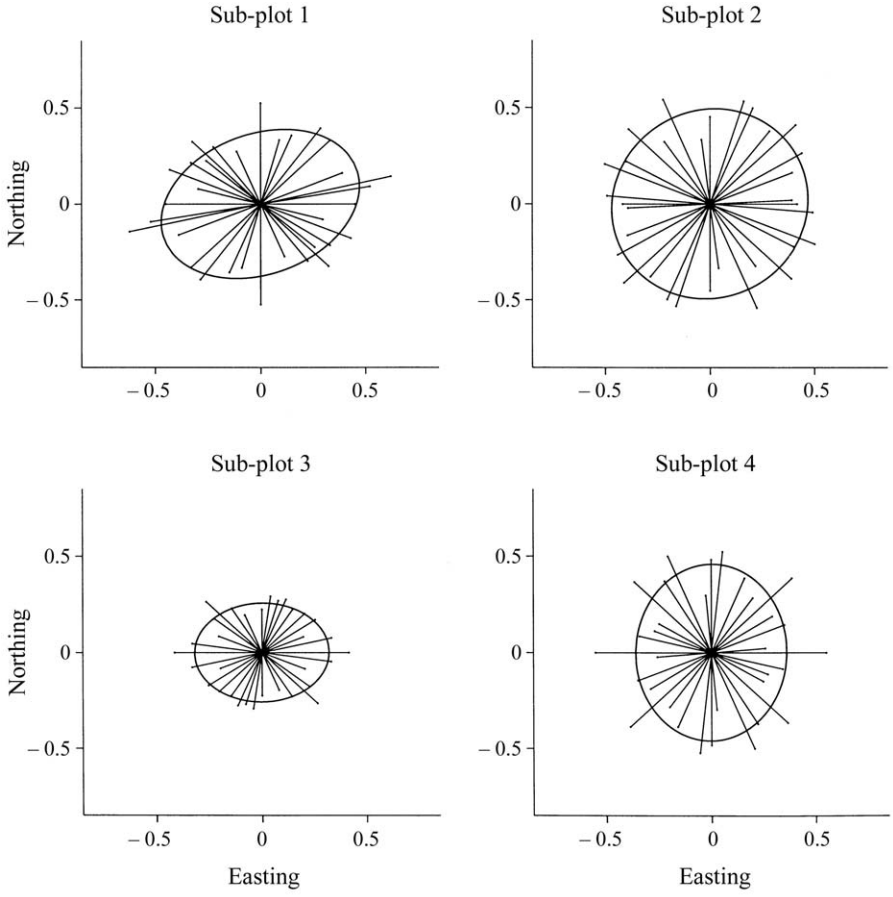

Figure 8. Ellipses fitted to the mean inter-boundary spacings on the four sub-plots at Aguas.

to south. In both, however, there is so much fluctation unaccounted for (almost 100%) that these apparent anisotropies are of little consequence.

4.3 *Marquesa and Hotel*

The analysis of the transect spacings from Marquesa and Hotel produced similar results, shown by the cumulative distributions (Fig. 3) and the associated statistics (Table 1). The pattern at Marquesa seems isotropic, but that at Hotel is distinctly anisotropic. The ellipse fitted to the mean spacings is the most eccentric of all; its anistropy ratio is 0.697 (Fig. 6). Here, we can be confident that this anisotropy is real with its orientation 123°. As for the Aguas site we can superimpose the envelope of the anisotropic model on cumulative frequencies, and this appears in Fig. 5b. The envelope is significantly wider than that for the Aguas site, Fig. 5a.

4.4 *Transitions*

Table 3 lists the estimated transition probabilities for the three main plots. The most striking feature of the matrices is their lack of symmetry. If we take the matrix for the Aguas site as an example (Table 3), we see that all of the transitions from classes of vegetation to bare soil exceed 0.5; none of the those from bare soil to particular species do. However, the transitions from bare soil to *S. tenacissima* (0.27) and even more so to *B. retusum* (0.39) are moderate. *Brachypodium retusum* is often next to *A. cytisoides* (0.30).

The transition probabilities for the sub-plots (Table 4) were similar to those for the whole plot, but with some fluctuation in the values from sub-plot to sub-plot. As for the whole plot, all of the transitions from classes of vegetation to bare soil exceed 0.5, but in three of the sub-plots the transition probabilities from bare soil to *B. retusum* are larger than in the plot as a whole: 0.40 for sub-plot 1, 0.45 for sub-plot 2, 0.44 for sub-plot 3. We estimated moderate probabilities for the transition between *S. tenacissima* and *B. retusum*: 0.15 on sub-plot 1, 0.17 on sub-plot 2, and 0.29 on sub-plot 3. The same was true for the

Table 3. Estimated transition probabilities and proportions of cover for the whole Aguas plot and for the Marquesa and Hotel plots.

		Vegetation Class						
Aguas		*St*	*Ga*	*Br*	*Ac*	*Bare*	*Other*	*Proportion*
	St	0	0.047	0.170	0.015	0.736	0.032	0.197
	Ga	0.082	0	0.072	0.021	0.800	0.026	0.051
	Br	0.123	0.030	0	0.068	0.754	0.025	0.159
	Ac	0.046	0.037	0.296	0	0.602	0.019	0.018
	Bare	0.273	0.170	0.386	0.071	0	0.101	0.517
	Other	0.089	0.041	0.098	0.016	0.756	0	0.057

		Vegetation Class				
Marquesa		*St*	*Ga*	*Bare*	*Other*	*Proportion*
	St	0	0.000	0.979	0.021	0.437
	Ga	0.000	0	0.971	0.029	0.038
	Bare	0.885	0.079	0	0.036	0.498
	Other	0.333	0.042	0.625	0	0.027

		Vegetation Class						
Hotel		*St*	*Ga*	*Br*	*Ac*	*Bare*	*Other*	*Proportion*
	St	0	0.004	0.216	0.000	0.749	0.032	0.379
	Ga	0.034	0	0.000	0.000	0.966	0.000	0.009
	Br	0.288	0.000	0	0.005	0.627	0.080	0.064
	Ac	0.000	0.000	0.125	0	0.875	0.000	0.003
	Bare	0.447	0.059	0.281	0.015	0	0.198	0.509
	Other	0.075	0.000	0.142	0.000	0.783	0	0.035

St = *Stipa tenacissima*, Ga = *Globularia alypum*, Br = *Brachypodium retusum*, Ac = *Anthyllis cytisoides*.

Table 4. Estimated transition probabilities and proportions of cover for the Aguas sub-plots.

		Vegetation class						
		St	*Ga*	*Br*	*Ac*	*Bare*	*Other*	*Proportion*
Sub-plot 1								
	St	0	0.072	0.145	0.012	0.699	0.072	0.112
	Ga	0.051	0	0.025	0.000	0.924	0.000	0.129
	Br	0.078	0.020	0	0.007	0.863	0.020	0.158
	Ac	0.125	0.000	0.125	0	0.750	0.000	0.004
	Bare	0.177	0.333	0.404	0.018	0	0.067	0.574
	Other	0.194	0.000	0.097	0.000	0.710	0	0.022
Sub-plot 2								
	St	0	0.009	0.173	0.009	0.755	0.055	0.241
	Ga	0.091	0	0.182	0.000	0.636	0.091	0.004
	Br	0.107	0.011	0	0.208	0.601	0.073	0.275
	Ac	0.020	0.000	0.755	0	0.224	0.000	0.025
	Bare	0.353	0.030	0.455	0.047	0	0.115	0.423
	Other	0.128	0.021	0.277	0.000	0.574	0	0.031
Sub-plot 3								
	St	0	0.000	0.289	0.026	0.684	0.000	0.059
	Ga	0.000	0	0.000	0.033	0.967	0.000	0.044
	Br	0.079	0.000	0	0.144	0.748	0.029	0.199
	Ac	0.013	0.013	0.263	0	0.697	0.013	0.082
	Bare	0.109	0.122	0.437	0.223	0	0.109	0.588
	Other	0.000	0.000	0.129	0.032	0.839	0	0.027
Sub-plot 4								
	St	0	0.000	0.045	0.136	0.591	0.227	0.461
	Ga	0.000	0	0.087	0.000	0.826	0.087	0.041
	Br	0.114	0.057	0	0.114	0.429	0.286	0.035
	Ac	0.300	0.000	0.100	0	0.600	0.000	0.036
	Bare	0.394	0.144	0.114	0.182	0	0.167	0.314
	Other	0.357	0.036	0.179	0.000	0.393	0	0.111

St = *Stipa tenacissima*, Ga = *Globularia alypum*, Br = *Brachypodium retusum*, Ac = *Anthyllis cytisoides*.

transition from *A. cytisoides* to *B. retusum*: 0.12 for sub-plot 1, 0.26 for sub-plot 3 and 0.10 for sub-plot 4; but on sub-plot 2 it was 0.8. The transitions from *G. alypum* to all other species are very small, and in particular we note that there are no transitions to *A. cytisoides* on sub-plots 1, 2 and 4, and to *S. tenacissima* on sub-plots 3 and 4. Table 3 lists the estimated transition probabilities for the Marquesa and Hotel sites. As at Aguas there are moderate transition probabilities from *S. tenacissima* to *B. retusum* and very small ones from *G. alypum* and the other species. The probabilities of transition from every species to bare soil are large, some remarkably close to 1, signifying that the species occur effectively as ''islands'' surrounded by bare ground.

4.5 *Geostatistical results*

To explore and test the geostatistical approach, we sampled the transects at short intervals (0.1 m) and computed for each site, and at Aguas the four sub-plots, the series of experimental values defined in Equation (10). We then fitted models by weighted least squares in which the weights were proportional to the numbers of paired comparisons, $m(h)$ in the equation, again using the FITNONLINEAR directive in GenStat (Payne *et al.*, 2002). The models we tried are three of the standard ones (see, e.g., Webster and Oliver, 2001) and are as listed below. In each c_0 is the intercept on the ordinate, c_1 is a spatially structured component equal to the upper bound of the function minus the intercept, and a or r is a distance parameter.

Spherical:

$$\begin{aligned} y &= c_0 + c_1\left\{\frac{3}{2}\left(\frac{h}{a}\right) - \frac{1}{2}\left(\frac{h}{a}\right)^3\right\}, \quad \text{for } 0 < h \leq a \\ &= c_0 + c_1, \quad \text{for } h > a \\ &= 0, \quad \text{for } h = 0. \end{aligned} \tag{13}$$

Pentaspherical:

$$\begin{aligned} \gamma(h) &= c_0 + c_1\left\{\frac{15}{8}\left(\frac{h}{a}\right) - \frac{5}{4}\left(\frac{h}{a}\right)^3 + \frac{3}{8}\left(\frac{h}{a}\right)^5\right\}, \quad \text{for } 0 < h \leq a \\ &= c_0 + c_1, \quad \text{for } h > a \\ &= 0, \quad \text{for } h = 0. \end{aligned} \tag{14}$$

Exponential:

$$y = c_0 + c_1\left\{1 - \exp\left(-\frac{h}{r}\right)\right\}. \tag{15}$$

Examples of these appear in Figs 9 and 10. The spherical and pentaspherical models increase almost linearly from their intercepts and then curve fairly tightly to reach their maxima at finite distances, a, which for each is the range of the model. The former curves more tightly than the latter. The exponential model curves gradually from its intercept and approaches its maximum asymptotically. It may be regarded as having an effective range at which the function reaches $c_0 + 0.95c_1$, and this is approximately $a' = 3r$ (Webster and Oliver, 2001).

Some of the results appear in Figs 9 and 10 in which the experimental values are plotted as points and the models of best fit in the least squares sense are shown by the continuous lines. Table 5 lists the models, their distance parameters and their equivalent effective ranges.

5. Discussion and conclusions

The results for these three sites suggest that the cumulative distributions functions of spacings between successive patch boundaries summarize well the patterns of patchiness

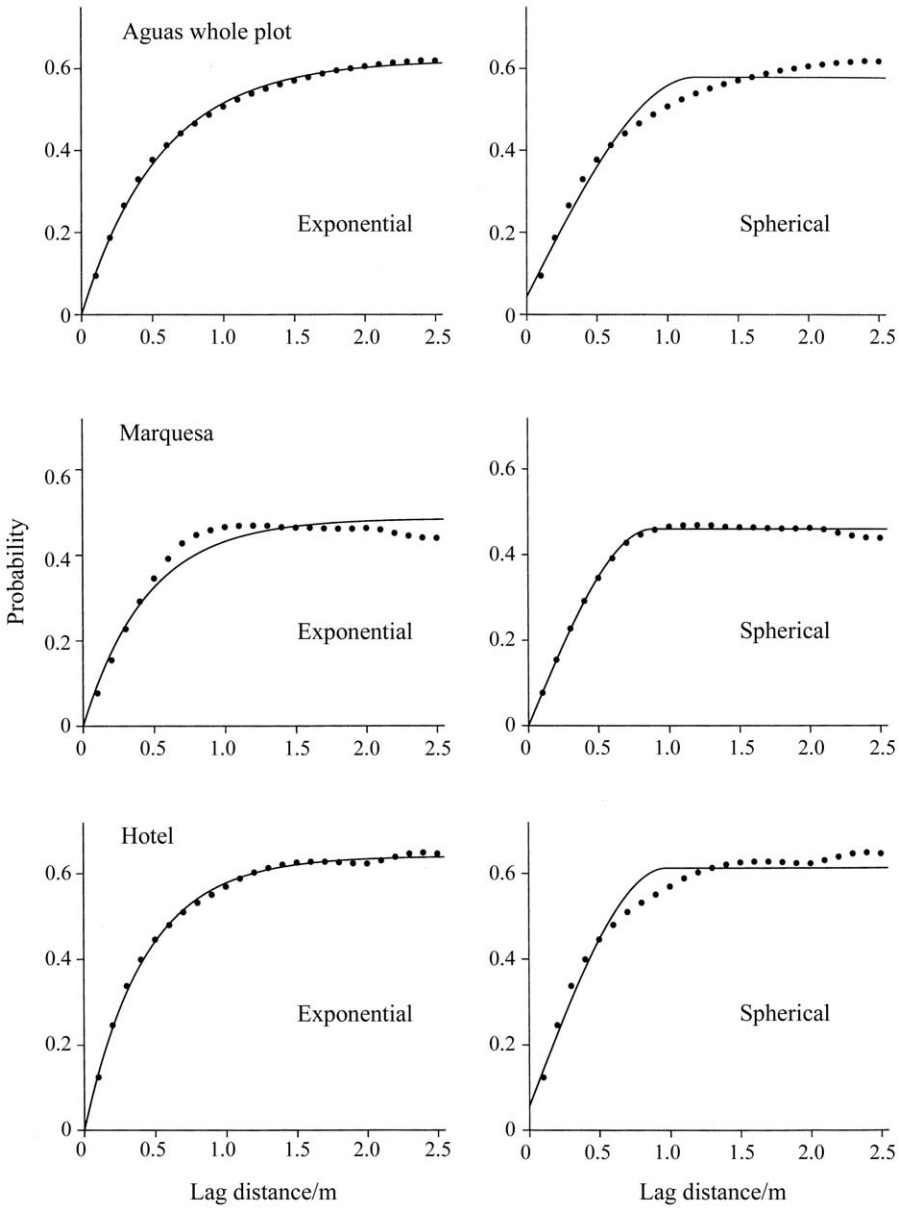

Figure 9. Calculated transition probabilities plotted against lag distance (point symbols) and the functions of best fit shown with solid lines for the three main plots. The types and parameters of the functions are listed in Table 4.

of the vegetation. The technique discriminates between the four strata identified intuitively at Aguas; there are substantial differences in the intensity parameter (reciprocal of mean inter-boundary spacing) of the distributions. Sub-region 3 has visibly the finest pattern, and sub-region 2 has the coarsest. The pattern on the Hotel plot and that on one of the sub-

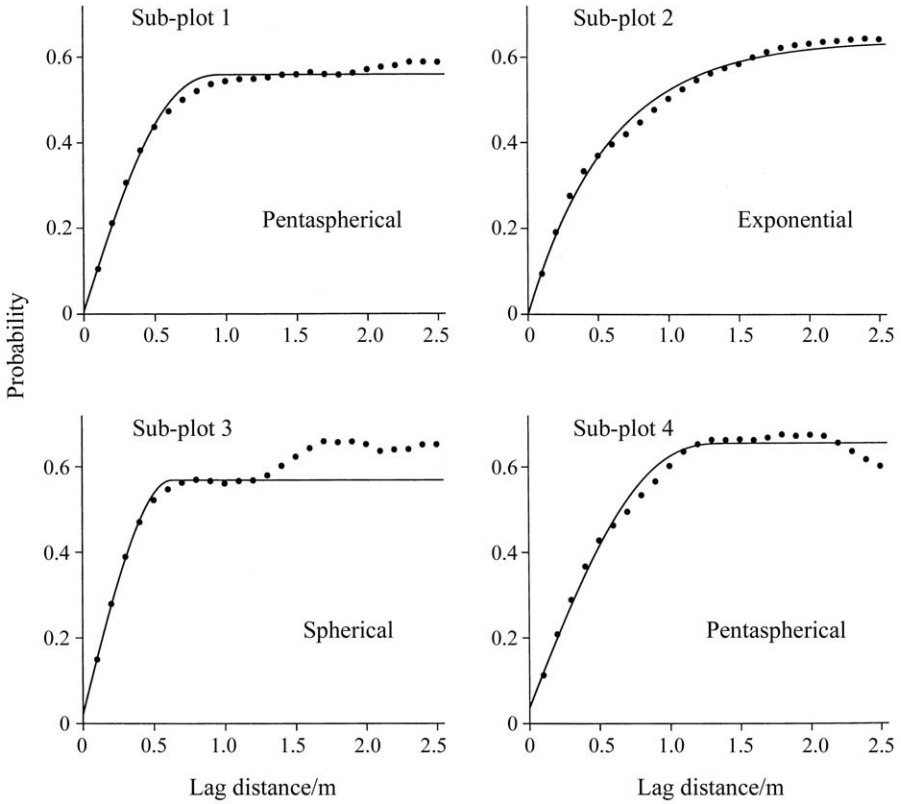

Figure 10. Calculated transition probabilities plotted against lag distance (point symbols) and the functions of best fit shown with solid lines for the four sub-plots at Aguas. The types and parameters of the functions are listed in Table 4.

plots at Aguas were anisotropic. It can also distinguish the differences between the different species that form the vegetation mosaic. The estimated transition probabilities suggested the presence of biotic interactions between the different species. The fact that the transitions from all the species individually to bare soil exceed 0.6 suggests that abiotic

Table 5. Models fitted to describe the spatial transition functions and their estimated distance parameters (in metres).

Plot	*Model*	*Distance Parameter*	*Effective Range*
Aguas whole plot	Exponential	0.561	1.682
Aguas sub-plots			
1	Pentaspherical	1.088	1.088
2	Exponential	0.591	1.772
3	Spherical	0.628	0.628
4	Pentaspherical	1.527	1.527
Marquesa	Spherical	0.886	0.886
Hotel	Exponential	0.428	1.285

factors, and in particular the availablity of water, constrain vegetation development and patterns.

Stipa tenacissima steppes are often structured in a spotty or banded spatial configuration (Puigdefábregas and Sánchez, 1996; Maestre and Cortina, 2002) with patterns like that of the ''tiger-bush'' in semi-arid Africa (Valentin *et al*., 1999). Many hypotheses have been put forward to explain the formation and maintenance of this particular pattern, but there is yet no consensus. Some authors have suggested that differences in soil can promote the formation of vegetated mosaics (Boaler and Hodge, 1962; Belsky, 1986). Valentin *et al*. (1999) suggested that the patterns are related to topography and in particular to slope. HilleRisLambers *et al*. (2001) suggest that there is a positive feedback between plant density and infiltration and that this is the main process determining the spatial pattern of semi-arid vegetation. Other authors argue that vegetated mosaics form solely as a result of the intrinsic dynamics of the vegetation itself (Thiéry *et al*., 1995; Lefever and Lejeune, 1997; Couteron and Lejeune, 2001) or by the combination of those dynamics and disturbances such as fire or grazing (Kellner and Bosch, 1992; Jeltsch *et al*., 1997; Bromley *et al*., 1997). Sánchez (1995) and Puigdefábregas and Sánchez (1996) think that the patterns of vegetation on the *S. tenacissima* steppes are determined by topography and the associated water fluxes. On moderate slopes *S. tenacissima* tussocks tend to be aligned parallel to the contours; this maximizes their ability to trap and store water and sediment and gives the appearance of the regular pattern. As the gradient steepens the patches of vegetation tend to become more broken as a consequence of increased runoff, and stripes develop downslope. The analysis for the Marquesa and Aguas sites showed no evident anisotropy. This suggests that the pattern develops to optimize the use of water in the soil (Puigdefábregas and Sánchez, 1996). Nevertheless, on the vegetation map of Aguas, the tussocks of *S. tenacissima* look somewhat elongated from north-west to south-east, whereas the patches of *B. retusum* seem elongated from west to east. The model we fitted to the pattern, however, encompassed all species, and returned as a result a non-significant anisotropy for the whole plot. On the Hotel plot, there was a significant anisotropy with a direction of maximum spacing of 124°. The slope there is similar to that at the other two sites, and the anisotropy found suggests that there are other factors that control the spatial pattern of the vegetation. The most likely explanation is the outcropping rock, which is elongated from north-west to south-east. These bands of rock almost certainly limit the growth of the tussocks to the spaces between them. They might also determine recruitment of plants to such spaces, resulting is the pattern we see.

Some interesting features of the plant communities in the regions we studied can be inferred from the transition matrices. Most patches of individual species are next to bare soil; thus we have two-phase mosaics composed of plant cover surrounded by bare ground. However, the varied transition probabilities between the species may reveal differences on the direction and intensity of biotic interactions. Transition probabilities from *A. cytisoides* to *B. retusum* and from *S. tenacissima* to *B. retusum* suggest a positive association between these species. *Anthyllis cytisoides* is a N_2-fixing legume that can improve soil conditions under its canopy (Bochet *et al*., 1999), and once established could enhance the growth of *B. retusum*. But it is also likely that well developed *B. retusum* patches could facilitate the establishment of *A. cytisoides* seedlings as a result of improved soil conditions and microclimate under its canopy as compared with those of the adjacent bare ground. Several studies have shown that *S. tenacissima* improves its own microenvironment, whether by ameliorating the microclimate (Maestre *et al*., 2001), improving the soil

structure (Bochet *et al*., 1999), increasing the amount of water stored in the soil (Puigdefábregas and Sánchez, 1996) and infiltration (Cerdá, 1997; Maestre *et al*., 2002), and increasing the availability of nutrients (Puigdefábregas and Sánchez, 1996). These changes allow *S. tenacissima* tussocks to facilitate the establishment of bryo-lichenic communities (Maestre, 2003; Maestre *et al*., 2002) and seedlings of woody shrubs (Maestre *et al*., 2001), and could also facilitate the development of *B. retusum*. Our results accord with those of García-Fayos and Gasque (2002) who found a positive association between several shrub species and *S. tenacissima* tussocks in semi-arid steppes of south east Spain. They contrast, however, with those obtained by Maestre and Cortina (2002), who reported a negative relationship between the spatial patterns of *S. tenacissima* and *B. retusum* at Aguas. This discrepancy may be due to differences in the data and methods between the latter and our study. Maestre and Cortina (2002) used as data cover values obtained from discrete sampling units (quadrats). This might result in a prevalence of pairwise negative associations, since those quadrats with large values of cover of one species will necessarily have small cover of the other species. On the other hand, the small transition probabilities between *G. alypum* and the other species might result from at least two factors; one is that *G. alypum* inhibits other species, and the other is that the seedlings of *G. alypum* have different requirements from those of the other species to establish. Further manipulative experiments are needed to elucidate the mechanisms responsible of the interactions suggested by our analyses.

The geostatistical approach, though providing an analysis of the distribution, does not estimate the distances between successive patch boundaries directly. Rather, what we get are distance parameters or effective ranges that we may try to interpret. Where the fitted probability function curves tightly, as it does with the spherical model, we get a range that approximates the mean boundary spacing (Aguas sub-plot 3 and Marquesa). The more gradually curving pentaspherical model has a range that exceeds the mean spacing; and the effective range of the gently curving exponential model overestimates the mean spacing substantially. The tight curvature of the spherical presumably arises because the patches are fairly similar in size, whereas the more varied spacings give rise to the exponential.

The methods introduced in this paper expand previous approaches for the spatial analysis of patchy vegetation based on the solely use of transition probabilities between patches (Pielou, 1967; Stowe and Wade, 1979). Our results suggest that they seem well able to describe the main features of the pattern of patchy vegetation. The cumulative curves of interboundary spacings give measures of the size distributions, and the ellipses fitted to the mean distances between boundaries record the degree of anisotropy and its direction. The estimated transition probabilities summarize the spatial arrangements between species, and between the plants and bare ground, and suggest interactions that can be explored further in detail. The methods introduced are likely to be valuable for comparing the spatial patterns of vegetation at many sites, and for evaluating temporal changes in the pattern at one or more sites. In addition, their mathematical background is less complicated than that underlying many other methods of spatial analysis, and the results obtained can be interpreted readily. Nevertheless, they have their shortcomings, which we can try to remove in the future. One is the lack of any tests on the transition probabilities: do the values differ significantly from the overall frequencies of occurrence of each plant type in the mosaic? A test such as that in Pielou (1967) could be useful if it were to lead to stronger inference about the interactions between the species suggested by transition probabilities.

Acknowledgments

We thank María Dolores Puche, José Huesca and Ángeles G. Mayor for help in the field, and Jordi Cortina, Susana Bautista and two referees for their valuable comments on earlier versions of our script. We also thank the Spanish Ministerio de Educación, Cultura y Deporte for its FPU grant to F.T. Maestre and the European Community for its support in the REDMED project under the Environment and Climate program (contract number ENV4-CT97-0682).

References

Aguiar, M.R. and Sala, O.E. (1999) Patch structure, dynamics and implications for the functioning of arid ecosystems. *Trends in Ecology and Evolution*, **14**, 273–77.

Belsky, A.J. (1986) Population and community processes in a mosaic grassland in the Serengeti, Tanzania. *Journal of Ecology*, **74**, 841–56.

Boaler, S.B. and Hodge, C.A.H. (1962) Vegetation stripes in Somaliland. *Journal of Ecology*, **50**, 465–74.

Bochet, E., Rubio, J.L., and Poesen, J. (1999) Modified topsoil islands within patchy Mediterranean vegetation in SE Spain. *Catena*, **38**, 23–44.

Bradshaw, G.A. and Spies, T.A. (1992) Characterizing canopy gap structure in forests using wavelet analysis. *Journal of Ecology*, **80**, 205–15.

Bromley, J., Brouwer, J., Barker, A.P., Gaze, S.R., and Valentin, C. (1997) The role of surface water redistribution in an area of patterned vegetation in a semi-arid environment, southwest Niger. *Journal of Hydrology*, **198**, 1–29.

Burgess, T.M. and Webster, R. (1984) Optimal sampling strategies for mapping soil types. I. Distribution of boundary spacings. *Journal of Soil Science*, **35**, 641–54.

Burgess, T.M. and Webster, R. (1986) A computer program for evaluating risks in constructing choropleth maps by point sampling on transects. *Computers and Geosciences*, **12**, 107–27.

Cammeraat, L.H. and Imeson, A.C. (1999) The evolution and significance of soil–vegetation patterns following land abandonment and fire in Spain. *Catena*, **37**, 107–27.

Cerdà, A. (1997) The effect of patchy distribution of *Stipa tenacissima* L. on runoff and erosion. *Journal of Arid Environments*, **36**, 37–51.

Couteron, P. and Lejeune, O. (2001) Periodic spotted patterns in semi-arid vegetation explained by a propagation–inhibition model. *Journal of Ecology*, **89**, 616–28.

Dale, M.R.T. (1999) *Spatial Pattern Analysis in Plant Ecology*, Cambridge University Press, Cambridge.

Dale, M.R.T. and Blundon, D.J. (1990) Quadrat variance analysis and pattern development during primary succession. *Journal of Vegetation Science*, **1**, 153–64.

Diggle, P.J. (1983) *Statistical Analysis of Spatial Point Patterns*, Academic Press, London.

Ford, E.D. and Renshaw, E. (1984) The interpretation of process from pattern using two-dimensional spectral analysis: modeling single species patterns in vegetation. *Vegetatio*, **56**, 113–23.

García-Fayos, P. and Gasque, M. (2002) Consequences of a severe drought on spatial patterns of woody plants in a two-phase mosaic steppe of *Stipa tenacissima* L. *Journal of Arid Environments*, **52**, 199–208.

Greig-Smith, P. (1983) *Quantitative Plant Ecology* (third edition), Blackwell Scientific Publications, Oxford.

Goovaerts, P. (1994) Study of spatial relationships between two sets of variables using multivariate geostatistics. *Geoderma*, **62**, 93–107.

Goovaerts, P. and Webster, R. (1994) Scale-dependent correlation between topsoil copper and cobalt concentrations in Scotland. *European Journal of Soil Science*, **45**, 79–95.

HilleRisLambers, R., Rietkerk, M., van den Bosch, F., Prins, H.H.T., and de Kroon, H. (2001) Vegetation pattern formation in semi-arid grazing systems. *Ecology*, **82**, 50–61.

Jeltsch, F., Milton, S.J., Dean, W.R.J., and van Rooyen, N. (1997) Simulated pattern formation around artificial waterholes in the semi-arid Kalahari. *Journal of Vegetation Science*, **8**, 177–88.

Kellner, K. and Bosch, O.J.H. (1992) Influence of patch formation in determining the stocking rate for southern African grasslands. *Journal of Arid Environments*, **22**, 99–105.

Lefever, R. and Lejeune, O. (1997) On the origin of tiger bush. *Bulletin of Mathematical Biology*, **59**, 263–94.

Le Houérou, H.N. (1986) The desert and arid zones of Northern Africa, in *The Ecosystems of the World. Hot Deserts and Arid Shrublands*, Volume 12B, M. Evenari, I. Noy-Meir and D.W. Goodall (eds), Elsevier Science, Amsterdam, pp. 104–47.

Maestre, F.T. (2003) Small-scale spatial patterns of two soil lichens in semi-arid Mediterranean steppe. *Lichenologist*, **35**, 71–81.

Maestre, F.T., Bautista, S., Cortina, J., and Bellot, J. (2001) Potential of using facilitation by grasses to establish shrubs on a semiarid degraded steppe. *Ecological Applications*, **11**, 1641–55.

Maestre, F.T. and Cortina, J. (2002) Spatial patterns of surface soil properties and vegetation in a Mediterranean semi-arid steppe. *Plant and Soil*, **241**, 279–91.

Maestre, F.T., Huesca, M., Zaady, E., Bautista, S., and Cortina, J. (2002) Infiltration, penetration resistance and microphytic crust composition in contrasted microsites within a Mediterranean semi-arid steppe. *Soil Biology and Biochemistry*, **34**, 895–8.

Ministerio de Medio Ambiente. (1999) *Estrategia Forestal Española*, Ministerio de Medio Ambiente, Madrid.

Müller, V. and Böttcher, J. (1987) Verteilung von Grenzabständen auf Bodenkarten und Ermittlung von Risikofunctionen. *Catena*, **14**, 561–70.

Payne, R.W. (ed.) (2002) *The Guide to GenStat, Part 2 Statistics*, VSN International, Oxford.

Pérez Cueva, J.A. (1994) *Atlas climático de la Comunidad Valenciana*, Conselleria de Obras Públicas, Urbanismo y Transportes, Valencia.

Pielou, E.C. (1964) A test for random mingling of the phases of a mosaic. *Biometrics*, **23**, 657–70.

Pielou, E.C. (1977) *Mathematical Ecology*, John Wiley & Sons, New York.

Platt, T. and Denman, K.L. (1975) Spectral analysis in ecology. *Annual Review of Ecology and Systematics*, **6**, 189–210.

Puigdefábregas, J. and Sánchez, G. (1996) Geomorphological implications of vegetation patchiness on semi-arid slopes, in *Advances in Hillslope Processes*, Volume 2, M.G. Anderson and S.M. Brooks (eds), John Wiley & Sons, Chichester, pp. 1027–60.

Sánchez, G. (1995) *Arquitectura y dinámica de las matas de esparto* (Stipa tenacissima *L.*)*, efectos en el medio e interacciones con la erosión*, Tesis doctoral, Universidad Autónoma de Madrid.

Stowe, L.G. and Wade, M.J. (1979) The detection of small-scale patterns in vegetation. *Journal of Ecology*, **67**, 1047–64.

Thiéry, J.M., d'Herbès, J.-M., and Valentin, C. (1995) A model simulating the genesis of banded vegetation patterns in Niger. *Journal of Ecology*, **83**, 497–507.

Valentin, C., d'Herbès, J.H., and Poesen, J. (1999) Soil and water components of banded vegetation patterns. *Catena*, **37**, 1–24.

Webster, R. and Oliver, M.A. (2001) *Geostatistics for Environmental Scientists*, John Wiley & Sons, Chichester.

Biographical sketches

Richard Webster is a soil scientist whose professional career spans more than four decades in Europe, Africa and Australia. He was Research Associate at Oxford University, led soil survey in Zambia and research on soil properties and composition at Rothamsted, and designed and analyzed soil survey with CSIRO in Australia. He has held research posts at the Ecole des Mines de Paris and in the Institut National de la Recherche Agronomique, France, and was Guest Professor at the Swiss Federal Institute of Technology in Zürich and Lausanne and at the Institute of Forestry, Snow and Landscape Research, also in Switzerland. He is currently Senior Research Fellow at Rothamsted and Visiting Professor in the University of Reading,

Fernando T. Maestre is a plant ecologist. After completing his doctorate at the University of Alicante he continued his research there until taking up his present position as Fulbright post-doctoral fellow in the Department of Biology at Duke University. His main research topics include the exploration of the role of environmental and organism heterogeneity on semi-arid ecosystem functioning and restoration, the evaluation of mechanisms of invasion by exotic species, and the analysis of the spatio-temporal dynamics of interactions, both positive and negative, between plant species.